PROCEEDINGS OF SPIE

SPIEDigitalLibrary.org/conference-proceedings-of-spie

Perfect reflection by dielectric subwavelength particle arrays: causes, implications, and technology

Magnusson, Robert, Ko, Yeong Hwan, Lee, Kyu Jin, Bootpakdeetam, Pawarat, Razmjooei, Nasrin, et al.

Robert Magnusson, Yeong Hwan Ko, Kyu Jin Lee, Pawarat Bootpakdeetam, Nasrin Razmjooei, Fairooz Abdullah Simlan, Ren-Jie Chen, Joseph Buchanan-Vega, Daniel J. Carney, Hafez Hemmati, Neelam Gupta, "Perfect reflection by dielectric subwavelength particle arrays: causes, implications, and technology," Proc. SPIE 11689, Integrated Optics: Devices, Materials, and Technologies XXV, 1168912 (5 March 2021); doi: 10.1117/12.2578953



Event: SPIE OPTO, 2021, Online Only

Perfect reflection by dielectric subwavelength particle arrays: Causes, implications, and technology

Robert Magnusson, Yeong Hwan Ko, Kyu Jin Lee, Pawarat Bootpakdeetam, Nasrin Razmjooei, Fairooz Abdullah Simlan, Ren-Jie Chen, Joseph Buchanan-Vega, Daniel J. Carney, Hafez Hemmati Department of Electrical Engineering, University of Texas Arlington, Arlington, Texas 76019, USA Neelam Gupta

DEVCOM Army Research Laboratory, 2800 Powder Mill Road, Adelphi, MD 20783, USA

ABSTRACT

Periodic arrays of resonant dielectric nano- or microstructures provide perfect reflection across spectral bands whose extent is controllable by design. At resonance, the array yields this result even in a single subwavelength layer fashioned as a membrane or residing on a substrate. The resonance effect, known as guided-mode resonance, is basic to modulated films that are periodic in one dimension (1D) or in two dimensions (2D). It has been known for 40 years that these remarkable effects arise as incident light couples to leaky Bloch-type waveguide modes that propagate laterally while radiating energy. Perfect reflection by periodic lattices derives from the particle assembly and not from constituent particle resonance. We show that perfect reflection is independent of lattice particle shape in the sense that it arises for all particle shapes. The resonance wavelength of the Bloch-mode-mediated zero-order reflectance is primarily controlled by the period for a given lattice. This is because the period has direct, dominant impact on the homogenized effective-medium refractive index of the lattice that controls the effective mode index experienced by the mode generating the resonance. In recent years, the field of metamaterials has blossomed with a flood of attendant publications. A significant fraction of this output is focused on reflectors with claims that local Fabry-Perot or Mie resonance causes perfect reflection with the leaky Bloch-mode viewpoint ignored. In this paper, we advance key points showing the essentiality of lateral leaky Bloch modes while laying bare the shortcomings of the local mode explanations. The state of attendant technology with related applications is summarized. The take-home message is that it is the assembly of particles that delivers all the important effects including perfect reflection.

Keywords: guided-mode resonance effect, leaky-mode resonance, resonant waveguide gratings, metamaterials, Bloch modes, wave propagation in periodic media, leaky-band dynamics, state of technology, metasurfaces

1. INTRODUCTION

The resonant optical lattices of interest in this study are made with periodic assemblies of arbitrarily shaped particles. These particles being pillars, blocks, or rods can be made of metals, dielectrics, and semiconductors. Whereas optical lattices are, in general, three-dimensional (3D), there are important variants in the form of 2D or 1D patterned films as treated here. Although the fundamental periodic element, namely the diffraction grating, has been around for more than 100 years, new solutions and applications based on spatially periodic modulations continue to appear. Related devices are often called metamaterials or metasurfaces and the like. Current lithographic technology enables fabrication of spatial modulations on subwavelength scales in one, two, or three dimensions. The resulting diffractive optical elements (DOE) or metasurfaces support waveguide modes if the refractive indices of the element are correctly chosen; these devices are often termed waveguide gratings in past literature. Waveguide modes that are guided or quasi-guided in waveguide gratings experience stopbands and passbands as the light frequency is varied. Nano- and microstructured lattices with subwavelength periodicity support guided-mode resonance effects and therefore represent fundamental building blocks for a host of device concepts. For many real-world applications, 1D and 2D photonic lattices exhibit attractive features such as compactness, minimal interface count, high efficiency, and potential monolithic fabrication with attendant robustness under harsh conditions. The fundamental resonance effects are available across the spectrum, from visible wavelengths to the microwave domain, by simple scaling of wavelength to period and proper materials selection.

*magnusson@uta.edu; phone 1 817 272-2672; fax 1 817 272-2253; www.leakymoderesonance.com

Integrated Optics: Devices, Materials, and Technologies XXV, edited by Sonia M. García-Blanco, Pavel Cheben, Proc. of SPIE Vol. 11689, 1168912 · © 2021 SPIE CCC code: 0277-786X/21/\$21 · doi: 10.1117/12.2578953

There are two main types of 1D and 2D photonic lattices in the class of metamaterials. The first type is built with isolated particles residing in a host medium that is often air. The second type consists of particles that rest on a layer that is made with the same material. Both types can support resonant quasi-guided modes that are induced by an external broadside incident electromagnetic wave [1-28]. Local Fabry-Perot and Mie mode signatures may be observable via computations within the structural particle geometry. Nevertheless, it has been shown that such local modes do not cause the high reflection observed computationally and experimentally in resonant photonic lattices with lateral Bloch modes providing the main properties [29]. Guided-mode resonance occurs at or near the second, or leaky, stop band. This band exhibits many remarkable physical properties including band transitions and bound states in the continuum [30]. Device concepts with experimental prototypes verifying theoretical predictions include wideband reflectors [25], nonfocusing spatial filters [26], ultra-sparse reflectors and polarizers [24], single-layer bandpass filters [27], multiparametric resonant sensors [28], and long-wave infrared resonant elements [31-33].

In this paper, we discuss the physical principles of resonant leaky-mode lattices. We review elementary facts related to diffractive optical elements and diffraction gratings as these constitute the original basis for metamaterials. We show that perfect reflection is obtainable in 1D and 2D lattices and that its occurrence is immune to particle shape. We review the leaky-mode band structure briefly and emphasize that its origin lies in the periodic assembly as opposed to particle resonance. The state of related technology is briefly summarized.

2. DIFFRACTIVE OPTICAL ELEMENTS: BASIS FOR METAMATERIALS

Classic diffractive optical elements (DOE) consist of regular spatial patterns arranged to control propagation of light. Lithographic patterning of dielectric surfaces, layers, or volume regions yields low-loss structures that affect the spatial distribution, spectral content, energy content, polarization state, and propagation direction of an optical wave. Common applications include spectral filters, diffractive lenses, antireflection surfaces, beam splitters, beam steering elements, laser mirrors, polarization devices, beam-shaping elements, couplers, and switches. These components are widely used in lasers, fiber-optic communication systems, spectroscopy, medical technology, integrated optics, imaging, and other optical systems.

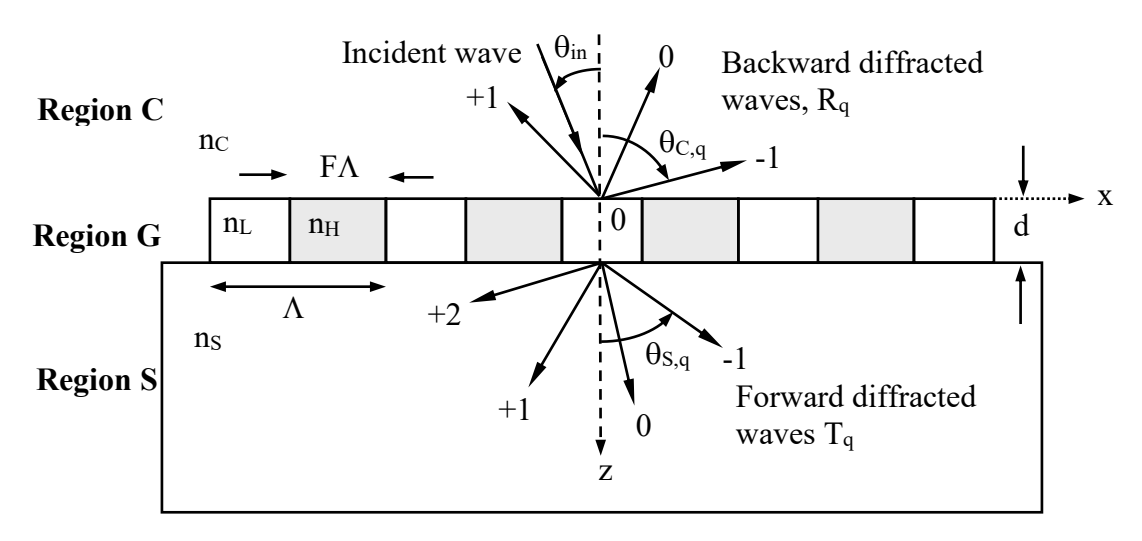


Figure 1. Geometry of diffraction by a canonical 1D rectangular grating with reflectance R and transmittance T.

The diffraction grating is the fundamental building block of diffractive optical elements. These may be planar or surfacerelief gratings made of dielectrics or metals. Figure 1 illustrates a single-layer diffraction grating and key descriptive parameters including the grating period, Λ , the grating fill factor, F, the grating refractive indices (n_H , n_L), thickness, d, and refractive indices of the cover and substrate media (n_C , n_S). The grating shown has a rectangular profile, if F=0.5 the profile is said to be square. An incident plane wave at angle θ_{in} is dispersed into several diffracted waves (diffraction orders labeled by the integer q as shown) propagating both forwards and backwards. The propagation angle of each diffracted wave may be obtained from the grating equation given by

$$n_{P} \sin \theta_{P,q} = n_{C} \sin \theta_{in} - q \lambda \Lambda \tag{1}$$

where λ is the free-space wavelength, q is an integer, and P is either C or S depending on the region under consideration. The grating equation is a universal equation that applies to all periodic DOEs no matter what the grating shape is. It is only the diffraction efficiency DE_q , representing the relative fractions of power carried by the various diffraction orders q, that is affected by the grating or particle shape. In the subwavelength regime, all higher diffraction orders are evanescent with only the q=0 orders propagating in the external regions. The grating equation is immune to particle shape in any diffraction regime such that the propagation directions of the output waves q>0 depend only on a single structural parameter namely the period Λ . The grating equation pertains to the assembly of particles.

Perfect reflection is another property of periodic lattices that derives from the particle assembly rather than from the constituent particles. Perfect reflection R_0 =1 is independent of lattice particle shape in the sense that it arises for all particle shapes. The resonance wavelength of the Bloch-mode-mediated zero-order reflectance at which R_0 =1 is primarily controlled by the period for a given lattice. This is because the period has direct, dominant effect on the homogenized effective-medium refractive index of the lattice. The effective index of a rectangular lattice such as that in Fig. 1 is provided by the Rytov formulation [34, 35]. For TE polarization, for example, the effective-medium index n_{TE}^{EMT} is found by

$$\sqrt{\mathbf{n}_{L}^{2} - (\mathbf{n}_{TE}^{EMT})^{2}} \tan \left[\frac{\pi \Lambda}{\lambda} (1 - F) \sqrt{\mathbf{n}_{L}^{2} - (\mathbf{n}_{TE}^{EMT})^{2}} \right] = -\sqrt{\mathbf{n}_{H}^{2} - (\mathbf{n}_{TE}^{EMT})^{2}} \tan \left[\frac{\pi \Lambda}{\lambda} F \sqrt{\mathbf{n}_{H}^{2} - (\mathbf{n}_{TE}^{EMT})^{2}} \right]$$
(2)

The explicit and primary dependence on the period is clear in Eq. 2 with the grating shape contributing via F. From this effective-medium theory (EMT) homogenized index, the final effective modal index seen by the lateral Bloch mode N_{eff} can then be found. If the period is fixed, variations in the resonance location are due to particle shape as it defines particle embodiment and contribution to the index. In the subwavelength diffraction regime, perfect reflection is immune to the grating shape since, in lossless periodic arrays at resonance, 100% reflection is possible no matter what the shape of the grating ridge. This discussion generalizes completely to 2D periodic lattices and gratings.

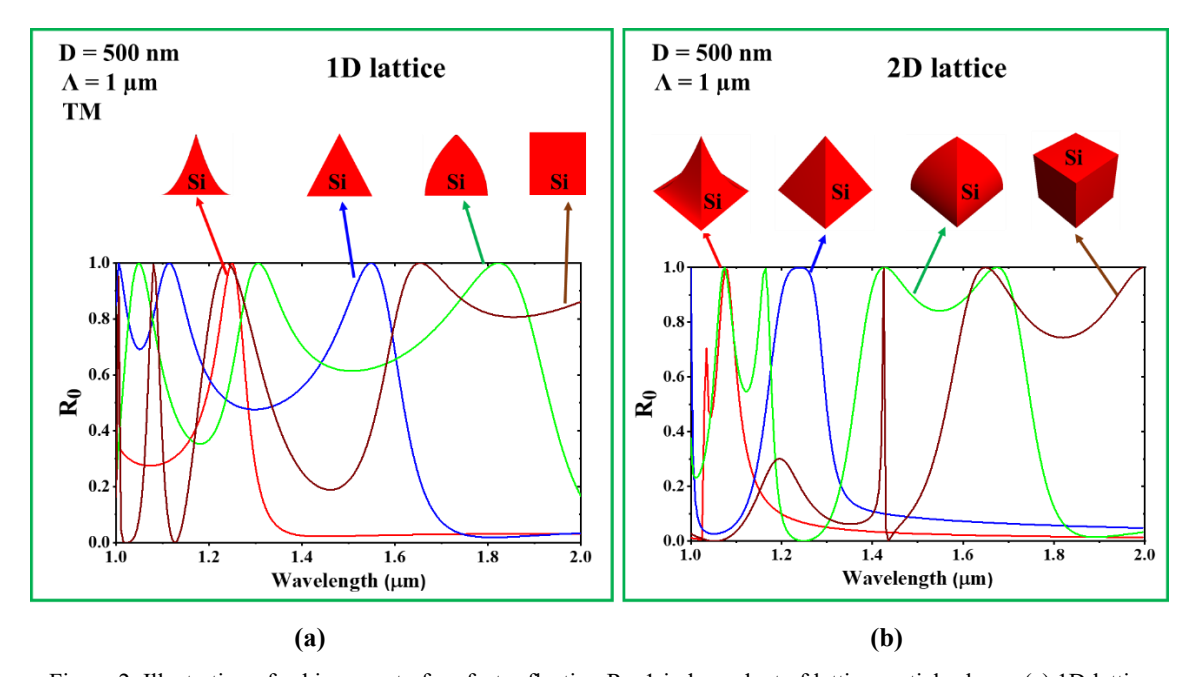


Figure 2. Illustration of achievement of perfect reflection R_0 =1 independent of lattice particle shape. (a) 1D lattice with grating ridge shape shown. (b) 2D lattice with particle shape noted. The lattices are made of silicon with air as host medium. For the case of fixed period in this example, the lateral Bloch modes propagating along these lattices see an effective mode refractive index N_{eff} that depends on the particle shape. Thus, the particle shape affects the resonance wavelength but not the condition R_0 =1 as seen in the figure.

The attainment of perfect reflection R_0 =1 is illustrated in Fig. 2 that shows zero-order reflectance R_0 spectra for some example particle shapes. Thus, immediately, based on these straightforward arguments, one would not expect local resonance effects, that depend strongly on the lattice constituent particle shape and refractive index, to be particularly significant in determining fundamental properties and functionality. Hence, one concludes that local Fabry-Perot (FP) or Mie resonances will not be governing the properties of periodic resonant metamaterials for either 1D or 2D modulation. In summary, it is the periodic system of particles that dominates the response providing all important effects and properties.

3. LEAKY-MODE LATTICE BAND STRUCTURE

Periodic assemblies of atoms and thin films exhibit diffraction and Bragg reflection. Associated stop bands and band gaps are well known. Kittel explains the band structure of atomic systems [36] while Yariv and Yeh treat the case of Bragg stacks [37]. Analogously, photonic lattices confined to layers as emphasized here, exhibit a band structure. This is because the lateral Bloch modes induced on resonance see a periodic structure as they propagate in the lattice. The leaky stop band plays crucial roles in operation of such lattices or metamaterials; hence we summarize key points of the band structure here. Clearly, the bands are associated with the assembly of particles and, again, local resonances do not play significant roles.

In direct connection with the discussion above, the reflector in Fig. 3(a) works under guided-mode resonance (GMR), which arises when the incident wave couples to a leaky Bloch waveguide mode by phase matching with the second-order grating [6,7,10,11]. For normal plane-wave incidence θ_{in} =0, counter-propagating leaky modes form a standing wave in the grating as indicated in Fig. 3(a). These waveguide modes interact with the grating and reradiate reflectively [11]. We show a schematic dispersion diagram in Fig. 3(b). The device works in the second (leaky) stop band corresponding to the second-order grating [13]. A given evanescent diffraction order can excite not just one but several leaky modes. Thus, in Fig. 3(b), we show the stop bands for the first two TE modes to emphasize this point. At each stop band, a resonance is generated as denoted in Fig. 3(b) also. The fields radiated by these leaky modes in a grating with a symmetric profile can be in phase or out of phase at the edges of the band [1,10]. At one edge, the phase difference is zero and hence the radiation is enhanced while at the other edge, there is a π phase difference inhibiting the radiation. If we let $\beta = \beta_R + i\beta_I$ be the complex propagation constant of the leaky mode, $\beta_I = 0$ at an edge signifies that no leakage is possible at that edge. One of the most common variety of resonance elements with rectangular profile and two-part period can only have symmetric profiles.

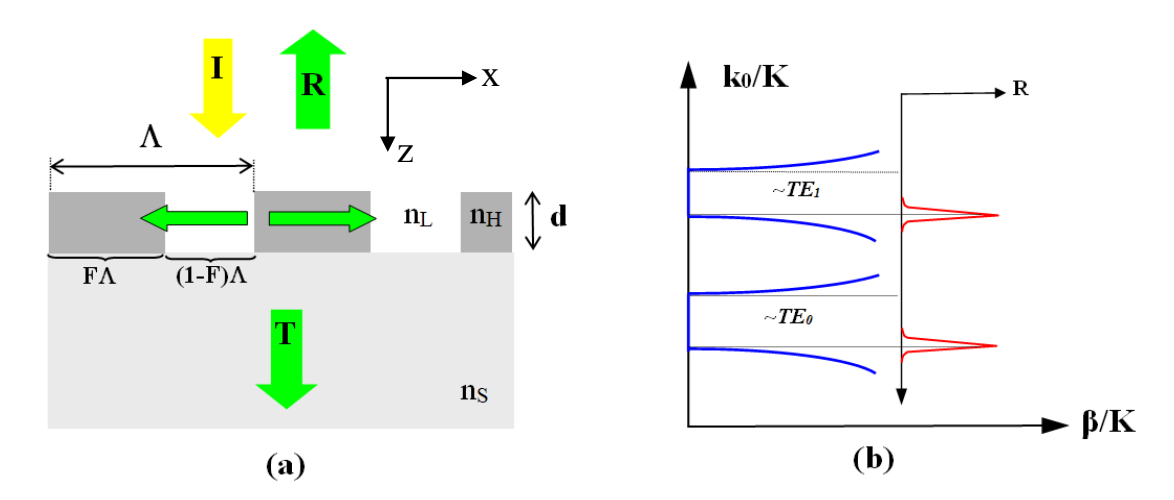


Figure 3. (a) A schematic view of a subwavelength guided-mode resonant lattice under normal incidence. A single silicon layer with thickness d, fill factor F, and a two-part period Λ is treated. When phase matching occurs between an evanescent diffraction order and a waveguide mode, a reflection resonance takes place. I, R, and T denote the incident wave, reflectance, and transmittance, respectively. (b) Schematic dispersion diagram of a GMR device at the leaky stop band. For a symmetric grating profile, a resonance appears at one edge. This picture applies to both TE (electric field vector normal to the plane of incidence) and TM (magnetic field vector normal to the plane of incidence) polarization states. $K = 2\pi/\Lambda$, $k_0 = 2\pi/\lambda$, and β is the propagation constant of a leaky mode.

The bands in Fig. 3(b) exhibit numerous interesting properties. The band structure admits a leaky edge and a non-leaky edge for each supported resonant Bloch mode if the lattice is symmetric. Depending on the device design, the leaky band edge can be placed under or above the band gap. The non-leaky edge is associated with what is now called a bound state in the continuum (BIC), or embedded eigenvalue, currently of considerable scientific interest [38-41]. It is possible to control the width of the leaky band gap by lattice design. In particular, as a modal band closes, there results a quasi-degenerate state—this state is remarkable as it is possible to transit to it by parametric and material choice. The transition to, and across, this point executes a band flip. The physical mechanisms inducing the band closure and the band flip are of fundamental interest. It can be shown that the frequency location of the leaky-mode resonance band edge, or the BIC edge, is determined by superposition of Bragg processes denoted by BR_{Q,m} where Q indicates the Bragg order and m denotes the Fourier harmonic of the dielectric constant modulation [30].

4. STATE OF TECHNOLOGY

The resonant optical lattices in play here are of interest for a host of possible applications. Numerous reports have appeared treating perfect reflection, often with good experimental results but with physical reasons claimed as FP or Mie resonance [42-47]. Our team has reported a wide array of resonant devices with diverse attributes over the decades. Figure 4(a) depicts a fabricated high-efficiency broadband reflector working under normal-incidence TM-polarized light. The measured reflectance spectrum exhibits ~490 nm bandwidth in the near-IR range with R₀>0.97 in the Si-on-Quartz materials system [48]. In 2019, as shown in Fig. 4(b), we reported a new class of metamaterial polarizers that are extremely compact and exhibit a record extinction ratio (ER) of 100,000 in the telecommunication spectral region [49]. These compact high efficiency polarizers can with additional R&D potentially serve as an alternative for conventional bulk polarizers that are in use presently in commercial products. We showed that in a dual-module resonant polarizer, the transmission of TE-polarized light is suppressed to values less than 10⁻⁵ (relative to input) while the TM transmission remains high due to the lossless, sparse nature of the polarizer. Figure 4(c) shows a fabricated wideband reflector comprising a Ge grating on a ZnS substrate and operating in the long-wave infrared (LWIR) spectral range [50]. The corresponding spectral response shows a resonant reflection band with R₀>90% spanning approximately 8.2-10.6 μm. Figure 4(d) outlines a recent journal paper [51] where we successfully report a high-quality resonant notch filter using a Ge grating on a ZnSe substrate for the 8-12 µm spectral range. Fourier-transform infrared spectrometry (FTIR) measurements of transmission show TE- and TM-polarized resonance notches at which T₀~0. These notches are located at 9.6 µm and 8.64 µm, respectively, and agree well with the theoretical spectra; at these resonance locations zero-order reflectance R₀~1 [51]. In Fig. 4(e), we theoretically demonstrate highly tunable LWIR filters that operate in a wide spectral range 5-14 µm with concurrently tuned central wavelengths and sidebands [52]. By optimizing an aperiodic zero-contrast grating (ZCG) grating on a wedged waveguide structure, the sidebands are simultaneously tuned along with the operational wavelength retaining constant spectral performance. Figure 4(f) depicts a commercial resonant grating biosensor reader along with microwell plates useful in many practical applications [53]. As a new approach to enhance Si Raman generation, we optimize GMR structures to operate two high-Q resonances matched to the nominal Raman shift of silicon that is 15.606 THz as depicted in Fig. 4(g).

5. CONCLUSIONS

In conclusion, we focus here on perfect reflection by resonant photonic lattices. Summarizing the classic diffractive optics view, we recall that the propagation directions external to periodic lattices are set by the period independent of grating profile. Analogously, the spectral map of perfect reflection is strongly influenced by the period. Classic diffractive effects lie at the heart of these devices and it is the assembly of particles, as opposed to the individual particle resonance, that yields all main properties. The lattices under study here are periodic and possess waveguide properties such that quasi-guided modes with finite lifetimes are sustained. We show that perfect reflection is independent of lattice particle shape in the sense that it arises for all particle shapes. The resonance wavelength of the Bloch-mode-mediated zero-order reflectance is primarily controlled by the period for a given lattice. This is because the period has direct, dominant effect on the homogenized effective-medium refractive index of the lattice that controls the effective mode index experienced by the lateral mode generating the resonance. Moreover, resonant photonic lattices exhibit a band structure. This is because the lateral Bloch modes induced on resonance see a periodic structure as they propagate in the lattice. The leaky stop band plays crucial roles in operation of such lattices or metamaterials. Clearly, the bands are associated with the assembly of particles and local resonances do not play significant roles. Finally, a snapshot of the state of relevant technology is furnished with some selected applications revealed.

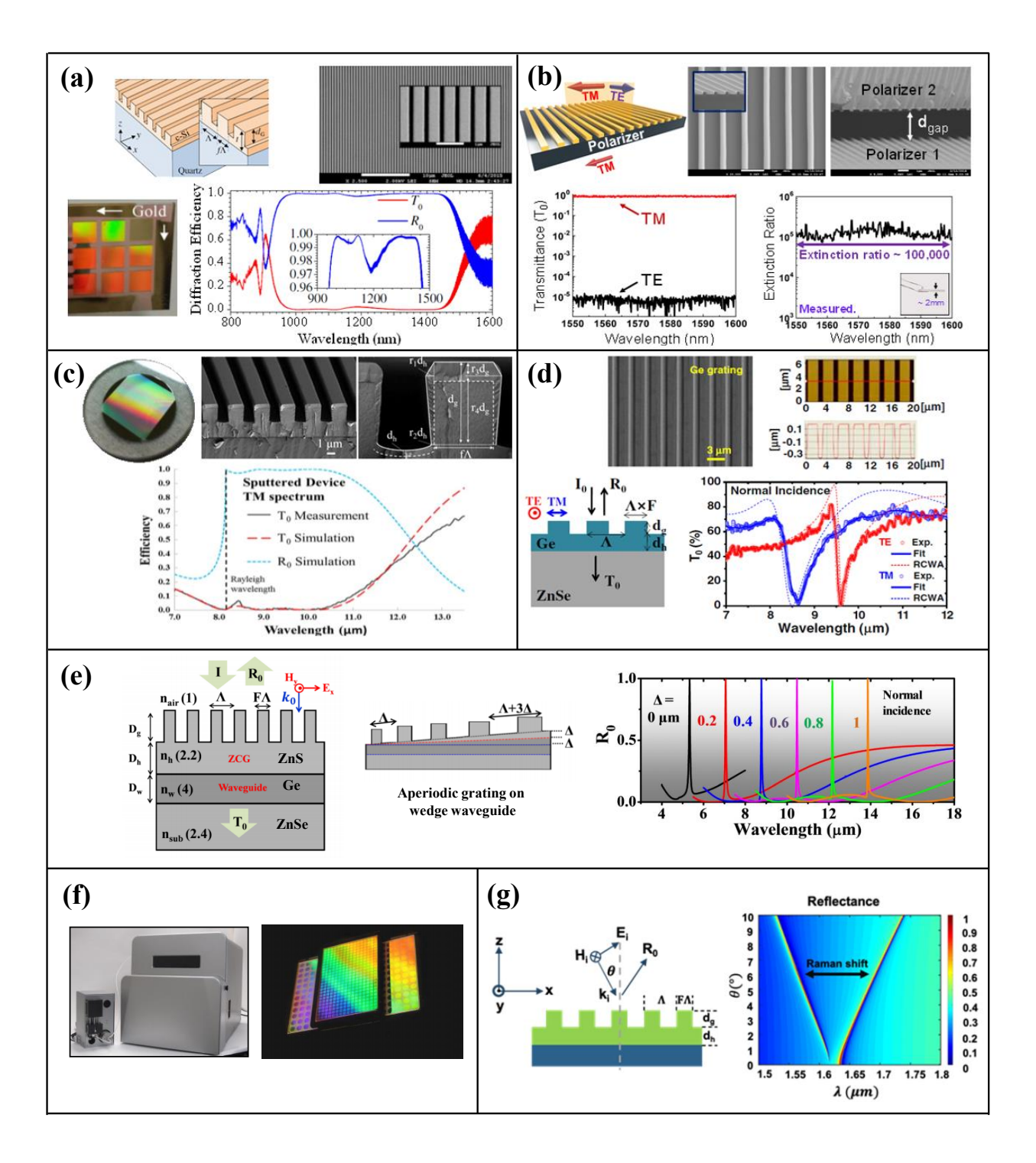


Figure 4. A snapshot of the state of the technology illustrating a collection of representative resonant devices and their spectral expressions and embodiments. (a) Near-IR wideband reflector, (b) near-IR high ER polarizer, (c) LWIR wideband reflector, (d) LWIR notch filter, (e) LWIR tunable filter, (f) GMR biosensor reader and plates, (g) Raman amplifier.

ACKNOWLEDGEMENTS

This research was supported, in part, by the UT System Texas Nanoelectronics Research Superiority Award funded by the State of Texas Emerging Technology Fund as well as by the Texas Instruments Distinguished University Chair in Nanoelectronics endowment. Additional support was provided by the National Science Foundation under Awards No. ECCS-1606898, ECCS-1809143, IIP-1826966 and Army Research Laboratory contract W911NF19-2-0171.

REFERENCES

- [1] P. Vincent and M. Neviere, "Corrugated dielectric waveguides: a numerical study of the second-order stop bands," Appl. Phys. 20, 345-351 (1979).
- [2] E. Popov, L. Mashev, and D. Maystre, "Theoretical study of the anomalies of coated dielectric gratings," Optica Acta 33, 607-619 (1986).
- [3] I. A. Avrutsky and V. A. Sychugov, "Reflection of a beam of finite size from a corrugated waveguide," J. Mod. Opt. 36, 1527-1539 (1989).
- [4] G. A. Golubenko, A. S. Svakhin, V. A. Sychugov, and A. V. Tishchenko, "Total reflection of light from a corrugated surface of a dielectric waveguide," Sov. J. Quantum Electron. 15, 886-887 (1985)
- [5] H. Kikuta, H. Toyota, and W. Yu, "Optical elements with subwavelength structured surfaces," Opt. Rev. 10, 63-73 (2003).
- [6] S. Wang and R. Magnusson, "Theory and applications of guided-mode resonance filters," Appl. Opt., 32, 2606-2613 (1993).
- [7] Y. Ding and R. Magnusson, "Resonant leaky-mode spectral-band engineering and device applications," Opt. Express 12, 5661-5674 (2004).
- [8] R. Magnusson and S. S. Wang, "New principle for optical filters," Appl. Phys. Lett. 61(9), 1022-1024 (1992).
- [9] W. Suh and S. Fan, "All-pass transmission or flattop reflection filters using a single photonic crystal slab," Appl. Phys. Lett. 84, 4905-4907 (2004).
- [10] R. F. Kazarinov and C. H. Henry, "Second-order distributed feedback lasers with mode selection provided by first-order radiation losses," IEEE J. Quantum Electron. QE-21, 144-150 (1985).
- [11] D. Rosenblatt, A. Sharon, and A. A. Friesem, "Resonant grating waveguide structures," IEEE J. Quantum Electron. 33, 2038-2059 (1997).
- [12] T. Tamir and S. Zhang, "Resonant scattering by multilayered dielectric gratings," J. Opt. Soc. Am. A 14, 1607-1616 (1997).
- [13] Y. Ding and R. Magnusson, "Band gaps and leaky-wave effects in resonant photonic-crystal waveguides," Opt. Express 15, 680-694 (2007).
- [14] D. Gerace and L. C. Andreani, "Gap maps and intrinsic diffraction losses in one-dimensional photonic crystal slabs," Phys. Rev. E 69, 056603 (2004).
- [15] S. T. Thurman and G. M. Morris, "Controlling the spectral response in guided-mode resonance filter design," Appl. Opt. 42, 3225-3223 (2003).
- [16] K. J. Lee, R. L. Comb, B. Britton, M. Shokooh-Saremi, H. Silva, E. Donkor, Y. Ding, and R. Magnusson, "Siliconlayer guided-mode resonance polarizer with 40-nm bandwidth," IEEE Photonics Technol. Lett. 20, 1857-1859 (2008).
- [17] R. Magnusson, D. Wawro, S. Zimmerman and Y. Ding, "Resonant photonic biosensors with polarization-based multiparametric discrimination in each channel," Sensors 11, 1476-1488 (2011).
- [18] H. Wu, J. Hou, W. Mo, D. Gao, and Z. Zhou, "A broadband reflector using a multilayered grating structure with multi-subpart profile," Appl. Phys. B 99, 519–524 (2010).
- [19] S. Peng and G. M. Morris, "Resonant scattering from two-dimensional gratings," J. Opt. Soc. Am. A 13, 993-1005 (1996).
- [20] R. Magnusson, "Wideband reflectors with zero-contrast gratings," Opt. Lett. 39, 4337-4340 (2014).
- [21] C. F. R. Mateus, M. C. Y. Huang, Y. Deng, A. R. Neureuther, and C. J. Chang-Hasnain, "Ultrabroadband mirror using low-index cladded subwavelength grating," IEEE Photon. Technol. Lett. 16, 518–520 (2004).
- [22] Mohammad J. Uddin, Tanzina Khaleque, and Robert Magnusson, "Guided-mode resonant polarization-controlled tunable color filters," Optics Express 22, 12307–12315 (2014).
- [23] Kyu J. Lee, James Curzan, Mehrdad Shokooh-Saremi, and Robert Magnusson, "Resonant wideband polarizer with single silicon layer," Applied Physics Letters 98, 211112-1–211112-3 (2011).

- [24] Jae Woong Yoon, Kyu Jin Lee, and Robert Magnusson, "Ultra-sparse dielectric nanowire grids as wideband reflectors and polarizers," Optics Express 23, 28849-28856 (2015).
- [25] Yeong Hwan Ko, Kyu Jin Lee, and Robert Magnusson, "Experimental demonstration of wideband multimodule serial reflectors," Optics Express 25, 8680-8689 (2017).
- [26] Manoj Niraula, Jae Woong Yoon, and Robert Magnusson, "Concurrent spatial and spectral filtering by resonant nanogratings," Optics Express 23, 23428-23435 (2015).
- [27] Manoj Niraula, Jae Woong Yoon, and Robert Magnusson, "Single-layer optical bandpass filter technology," Optics Letters 40, 5062-5065 (2015).
- [28] Robert Magnusson, Debra Wawro, Shelby Zimmerman, and Yiwu Ding, "Resonant Photonic Biosensors with Polarization-based Multiparametric Discrimination in Each Channel," Sensors: Special Issue Optical Resonant Sensors 11, 1476–1488 (2011).
- [29] Yeong Hwan Ko and Robert Magnusson, "Wideband dielectric metamaterial reflectors: Mie scattering or leaky Bloch mode resonance?," Optica 5, 289-294 (2018).
- [30] Sun-Goo Lee and Robert Magnusson, "Band flips and bound-state transitions in leaky-mode photonic lattices," Phys. Rev. B 99, 045304 (2019).
- [31] K. J. Lee, Y. H. Ko, N. Gupta and R. Magnusson, "Unpolarized resonant notch filters for the 8–12 μm spectral region," Opt. Lett. 45, 4452-4455 (2020).
- [32] Y. H. Ko, N. Gupta and R. Magnusson, "Resonant filters with concurrently tuned central wavelengths and sidebands," Opt. Lett. 45, 6046-6049 (2020).
- [33] N. Gupta and M. S. Mirotznik, "Performance Characterization of tunable longwave infrared filters using quantum cascade laser," Opt. Eng. 57, 127101 (2018).
- [34] S. M. Rytov, "Electromagnetic properties of a finely stratified medium," Sov. Phys. JETP 1956, 2(3) 466-475.
- [35] H. Hemmati and R. Magnusson, "Applicability of Rytov's Full Effective-Medium Formalism to the Physical Description and Design of Resonant Metasurfaces," ACS Photonics 7, 3177-3187 (2020).
- [36] C. Kittel, <u>Introduction to Solid State Physics</u>, 4th edition, Wiley 1971.
- [37] A. Yariv and P. Yeh, Photonics, 6th edition, Oxford University Press 2007.
- [38] A. Kodigala, T. Lepetit, Q. Gu, B. Bahari, Y. Fainman, and B. Kanté, "Lasing action from photonic bound states in continuum," Nature 541, 196–199 (2017).
- [39] J. Gomis-Bresco, D. Artigas and L. Torner, "Anisotropy-induced photonic bound states in the continuum," Nature Photonics 11, 232-236 (2017).
- [40] C. W. Hsu, B. Zhen, A. D. Stone, J. D. Joannopoulos, and M. Soljacic, "Bound states in the continuum", Nature Reviews Materials 1, 1–13 (2016).
- [41] D. C. Marinica, A. G. Borisov, and S. V. Shabanov, "Bound states in the continuum in photonics," Phys. Rev. Lett. 100, 183902 (2008).
- [42] P. Qiao, W. Yang, and C. J. Chang-Hasnain, "Recent advances in high-contrast metastructures, metasurfaces, and photonic crystals," Adv. Opt. Photon. 10, 180-245 (2018).
- [43] V. Karagodsky, C. Chase, and C. J. Chang-Hasnain, "Matrix Fabry-Perot resonance mechanism in high-contrast gratings," Opt. Lett, 36, 1704-1706 (2011).
- [44] Y. Huang, H. Xu, Y. Lu, and Y. Chen, "All-dielectric metasurface for achieving perfect reflection at visible wavelengths," J. Phys. Chem. C 122, 2990–2996 (2018).
- [45] A. I. Kuznetsov, A. E. Miroshnichenko, M. L. Brongersma, Y. S. Kivshar, and B. Luk'yanchuk, "Optically resonant dielectric nanostructures, "Science 354, 846 (2016).
- [46] C. Park, I. Koirala, S. Gao, V. R. Shrestha, S.-Shin Lee, and D. Yong Choi, "Structural color filters based on an all-dielectric metasurface exploiting silicon-rich silicon nitride nanodisks," Opt. Express 27, 667-679 (2019).
- [47] P. Moritra, B. A. Slovick, Z. G. Yu, S. Krishnamurthy, and J. Valentine, "Experimental demonstration of a broadband all-dielectric metamaterial perfect reflector," Appl. Phys. Lett. 104, 171102 (2014).
- [48] Manoj Niraula and Robert Magnusson, "Unpolarized resonance grating reflectors with 44% fractional bandwidth," Opt. Lett. 41, 2482-2485 (2016).
- [49] Hafez Hemmati, Pawarat Bootpakdeetam, and Robert Magnusson, "Metamaterial polarizer providing principally unlimited extinction," Opt. Lett. 44, 5630-5633 (2019).
- [50] Daniel J. Carney and Robert Magnusson, "Fabrication techniques for mid-IR resonant devices," Opt. Lett. 43, 5198-5201 (2018).
- [51] K. J. Lee, Y. H. Ko, N. Gupta, and R. Magnusson, "Unpolarized resonant notch filters for the $8-12\,\mu m$ spectral region," Opt. Lett. 45, 4452-4455 (2020).

- [52] Y. H. Ko, N. Gupta, and R. Magnusson, "Resonant filters with concurrently tuned central wavelengths and sidebands," Opt. Lett. 45, 6046-6049 (2020).
- [53] M. G. Abdallah, J. A. Buchanan-Vega, K. J. Lee, B. R. Wenner, J. W. Allen, M. S. Allen, S. Gimlin, D. W. Weidanz and R. Magnusson, "Quantification of Neuropeptide Y with Picomolar Sensitivity Enabled by Guided-Mode Resonance Biosensors" Sensors, 20, 126, 2020.